Meningeal γδ T cell-derived IL-17 controls synaptic plasticity and short-term memory

Miguel Ribeiro[#1], **Helena C. Brigas**[#1], **Mariana Temido-Ferreira**[1], **Paula A. Pousinha**[2], **Tommy Regen**[3], **Cátia Santa**[4,5], **Joana E. Coelho**[1], **Inês Marques-Morgado**[1], **Cláudia Valente**[1], **Sara Omenetti**[6], **Brigitta Stockinger**[6], **Ari Waissman**[3], **Bruno Manadas**[4], **Luísa V. Lopes**[1], **Bruno Silva-Santos**[1], **Julie C. Ribot**[1]

[1]Instituto de Medicina Molecular, Faculdade de Medicina, Universidade de Lisboa, Lisboa, Portugal

[2]Institut de Pharmacologie Moléculaire et Cellulaire, Centre National de la Recherche Scientifique, Université de Côte d'Azur, Nice, France

[3]Institute for Molecular Medicine, University Medical Center of the Johannes Gutenberg-University Mainz, Germany

[4]Center for Neuroscience and Cell Biology, Universidade de Coimbra, Coimbra, Portugal

[5]Institute for Interdisciplinary Research, Universidade de Coimbra, Coimbra, Portugal

[6]The Francis Crick Institute, London, UK

[#] These authors contributed equally to this work.

Abstract

The notion of "immune privilege" of the brain has been revised to accommodate its infiltration, at steady state, by immune cells that participate in normal neurophysiology. However, the immune mechanisms that regulate learning and memory remain poorly understood. Here we show that non-inflammatory IL-17 derived from a previously unknown foetal-derived meningeal-resident γδ T cell subset promotes cognition. When tested in classical spatial learning paradigms, mice lacking γδ T cells or IL-17 displayed deficient short-term memory, while retaining long-term memory. The plasticity of glutamatergic synapses was reduced in the absence of IL-17, resulting in impaired long-term potentiation in the hippocampus. Conversely, IL-17 enhanced glial cell production of brain derived neurotropic factor, whose exogenous provision rescued the synaptic and behavioral phenotypes of IL-17-deficient animals. Altogether, our work provides new clues on

the mechanisms that regulate short-term versus long-term memory and on the evolutionary and functional link between the immune and nervous systems.

Introduction

Neuroimmune interactions in the central nervous system (CNS) were until recently thought to be limited to cases of pathological insult (1). Among the important players that have been depicted to interact with the inflamed CNS, a particular attention has been paid to conventional CD4+ αβ T cells but also unconventional γδ T cells. In striking contrast to the former, which can take up to 5-7 days to clonally expand and differentiate into effector (« T helper ») subsets under the influence of specific "polarizing" cytokines (2), we and others have shown that murine γδ T cells are developmentally programmed in the thymus in the absence of overt inflammation, i.e. in the steady-state (3–5). This allows them to accumulate as effector lymphocytes in peripheral tissues and respond to challenge (such as infection) much more rapidly than their αβ T cell counterparts, i.e. within a time frame that aligns with innate immunity (6).

In the murine thymus, γδ T cells are programmed into two main effector subsets that produce either interferon γ (IFN-γ) or interleukin 17 (IL-17), and which can be further distinguished on the basis of various cell surface markers, such as CD27 (3) or CCR6 (7), among others (8). Important data have highlighted a critical role for both IFN-γ and IL-17 producing γδ T cells in neuroinflammation: IFN-γ producing γδ T cells were shown to mediate demyelination upon coronavirus infection (9), while IL-17-producing γδ T cells were found at high frequency in the brain of mice with experimental autoimmune encephalomyelitis (EAE) and to contribute to disease development (10). This latter subset has also been shown to have a key impact in the progression of cerebral ischemia-reperfusion injury (11). In both cases, IL-17 producing γδ T cells (abbreviated to γδ17 T cells from hereonin) have been pointed as critical players in disease progression, by contributing to a local immune amplification loop within the brain meningeal spaces and altering the stromal microenvironment of the inflamed brain, ultimately leading to blood-brain barrier (BBB) disruption (12, 13).

In stark contrast with their pathogenic role in neuroinflammation, γδ17 T cells are known to constitute a major source of IL-17 in various other non-lymphoid tissues at steady state, which interestingly contributes to normal tissue physiology, as illustrated by recent works reporting their key functions in bone repair (14) and thermogenesis (15). This is an interesting nascent field that may reveal novel physiological roles for γδ17 T cells residing in other tissues.

While the CNS has been regarded for decades as an immune privileged organ, shielded by the BBB, current neuroimmunology now acknowledges that lymphatic vessels within the dural sinuses of the meninges establish direct communication with the draining cervical lymph nodes (LNs) (16, 17) ; and that the immune system is crucial to support brain homeostasis and plasticity in a disease-free context. This stems from data establishing key roles for immune cells, particularly CD4^{+} αβ T cells, in physiological brain functions, including social behavior (18), sensory response (19) and spatial learning (20). Namely,

previous studies have demonstrated that T cell deficient mice display an impaired spatial memory when compared with wild-type (WT) controls, which could be restored after injection of WT splenocytes (21). Moreover, it has been reported an accumulation of IL-4 producing CD4+ αβ T cells in the meningeal spaces of the murine brain upon cognitive performance (22). This would benefit the learning capacity by inducing astrocytic expression of Brain Derived Neurotrophic factor (BDNF) and skewing the meningeal macrophages towards an anti-inflammatory profile (22). By contrast, pro-inflammatory cytokines such as IFN-γ and TNF-α have been shown to exert a negative effect on cognitive behavior (23, 24). Thus, it is tempting to assume that anti-inflammatory cytokines would support physiological brain function, whereas typical pro-inflammatory signals would hinder it, but this view may well be too simplistic.

Here, inspired by their important pathophysiological roles in brain inflammation (25), we hypothesized that innate-like γδ T cells might also contribute to neurophysiology in the steady state. We show that γδ T cells are a major source of IL-17 in the brain meninges at steady-state and promote short-term memory in naive mice by increasing glutamatergic synaptic plasticity of hippocampal neurons.

Results

Foetal-derived γδ T cells infiltrate the meninges since birth

We started this study by analysing by flow cytometry the immune content of meningeal infiltrates from naïve C57/BL6 mice throughout ontogeny. We found a sizeable population of highly proliferative and differentiated γδ T cells in the meningeal spaces already at birth and persisting throughout life, whereas their αβ T cell counterparts tended to accumulate after weaning (Fig. 1A-C). Meningeal γδ T cells displayed a particularly activated phenotype, enriched for CD69+ CD44hiCD62L- cells and scored nearly 100% of proliferating cells by Ki67 staining (Fig. 1D). Their repertoire was mostly restricted to the usage of the gamma chain variable region (Vγ) 6 of the T Cell Receptor (TCR) (Fig. 1E), characterizing a foetal thymic-derived population reported to colonize various non-lymphoid tissues (26, 27). Consistent with their foetal origin, meningeal γδ T cells were very poorly reconstituted upon transplantation of adult bone marrow precursors into irradiated C57/BL6 mice (Fig 1F). These data reveal a population of foetal-derived Vγ6-biased γδ T cells displaying an activated phenotype in the brain meninges at steady-state.

Meningeal γδ T cells are strongly biased towards IL-17 production

To further characterize the phenotype of meningeal γδ T cells, we focussed on their effector profile. We found that they displayed signatures of *bona-fide* IL-17-producing γδ (γδ17) T cells (3, 7) such as the expression of the master transcription factor RORγt and the chemokine receptor CCR6 (Fig. 2A-B). Consistently, a large fraction (~50%) of γδ T cells from the meninges of adult mice expressed IL-17 (but not IFN-γ) *ex vivo* (Fig. 2C), which was striking even compared to other tissues enriched in Vγ6+ γδ T cells (Fig. S1). Of note, IL-17+ cells were absent in the brain parenchyma (Fig. S2) and restricted to the meninges, where they were accounted almost exclusively by γδ T cells (Fig. 2D), whereas αβ T cells mostly provided IFN-γ (Fig. 2C). Most importantly, we confirmed these meningeal

phenotypes using an IL-17-eYFP fate mapping reporter mouse model (28) (Fig. 2E), which allows the detection of IL-17 producers while bypassing the need for *ex vivo* stimulation. Interestingly, most YFP+ γδ T cells co-expressed intracellular IL-17 protein, thus demonstrating their active functionality in the meninges (Fig. 2E).

Meningeal γδ17 T cells peaked after the first week of life (Fig. 2F) and, consistent with their Vγ6$^+$ phenotype (Fig. 1E) and proposed foetal origin (26), could not be efficiently generated by adult bone marrow precursor transplantation (Fig 2G).

Meningeal γδ T cell homeostasis is independent of inflammatory signals

To gain further insight on the potential mechanisms responsible for meningal γδ T cell accumulation and maintenance, we analysed mice deficient for specific components that could theoretically influence this process. Critically, we observed that meningeal γδ17 T cells were similarly abundant in germ-free (GF) and specific pathogen-free (SPF) mice; or after treatment of SPF animals with an antibiotic cocktail (Fig. 3A-B). Thus, resident meningeal γδ17 T cells at steady state are independent of commensal microbiota, contrary to pathogenic γδ17 T cells that migrate from the gut to the CNS in a mouse model of ischemic brain injury (12). Furthermore, the accumulation of γδ17 T cells in the meninges was independent of the pro-inflammatory cytokines IL-1β and IL-23 (Fig. 3C), known to drive their expansion in autoimmune pathology including EAE (10). Typical Pathogen Associated Molecular Patterns (PAMP) signals were also not required, as mice deficient for TLR2, TLR4, Caspase-1 or NOD1 harboured normal meningeal γδ17 T cell pools (Fig. 3D). These data collectively identify a non-inflammatory γδ17 T cell subset that populates the brain meninges in the perinatal period and persists throughout life.

γδ T cells producing IL-17 are required for short-term memory

Since they do not penetrate the brain parenchyma in the steady state (Fig. S3), T cells are thought to exert their effects on cognition through the secretion of soluble factors from the meninges (1, 29). To address the role of IL-17 produced by meningeal γδ T cells in this process, we analysed the behavior of mice deficient for IL-17 (IL-17-/-) or γδ T cells (TCRδ-/-) in classical neuroscience paradigms assessing spatial reference memory. Importantly, these mice had a normal exploratory behavior and did not show any particular signs of motor deficit or anxiety (Fig. S3-4). Strikingly, when tested on the Y-maze paradigm for short-term spatial working memory, IL-17-/- and TCRδ-/- mice displayed clear cognitive impairments, as they failed to prefer the novel arm, in contrast to inbred IL-17+/+ and TCRδ+/+ littermate controls (Fig. 4A-B and Fig S5A) or to C57BL/6 WT mice (Fig. S5B and S6). These IL-17 dependent short-term memory deficits were observed in both males (Fig. 4A-B, Fig.5A-B) and females (Fig. S6). Of note, we excluded a potential influence of the gut flora by showing that animals deficient for IL-17 or γδ T cells and respective WT littermate controls share similar microbiome compositions (Fig. S7). We further validated our findings in bone marrow chimeras (BMC) mostly devoid of meningeal γδ17 T cells (Fig. 2G), which displayed normal motor function and exploratory behavior (Fig. S3C, S4C), but impaired short-term learning (Fig. 4C and Fig. S5C).

To test the local impact of meningeal IL-17, we neutralized IL-17 *in situ* by injecting specific blocking monoclonal antibodies through the intra-cerebro-ventricular (ICV) route. Administrated to WT mice 24 hours before behavioral tests, this treatment abrogated short-term memory in the Y-maze (Fig. 4D).

Interestingly, IL-17-/-, TCRδ-/- and BMC mice showed normal behavior in the Morris Water Maze (MWM), the prototypic paradigm for long-term spatial reference memory, in which mice were tested in 4 trials/ day over a 4-day period, followed by a "probe" test at day 5 (Fig 4E and Fig. S8). To rule out different degrees of motivation and performance demand in the MWM *versus* the Y-maze, we adapted both paradigms to assess cognition in short-term and long-term timeframes, respectively (30, 31). Importantly, we confirmed in these re-designed experimental settings that both males and females deficient for IL-17 or γδ T cells suffer from short-term, but not long-term, memory deficits (Fig. 4F-H and Fig. S9-10 S10-11).

IL-17 modulates synaptic plasticity and AMPA/NMDA ratio upon a short-term memory task

As a first and unbiased assessment of the molecular mechanisms underlying the impact of meningeal γδ T cell-derived IL-17 on learning and memory, we used a quantitative SWATH-MS proteomics approach to compare the levels of hippocampal proteins between WT and IL-17-/- animals after Y-maze training. While changes in the expression of individual proteins were rather mild (Table S1), a broader look using pathway enrichment analysis (KEGG) pointed towards changes in synaptic plasticity, such as Long Term Potentiation (LTP), calcium signalling and glutamatergic synapse (32) (Fig. S11-12). To functionally address the impact of IL-17 deletion on synaptic plasticity, we examined baseline synaptic transmission and LTP in IL-17-/- and WT animals. Consistent with our hypothesis, IL-17-/- animals displayed impaired LTP specifically after a short-term Y-maze training (but not at steady state) (Fig. 5A-B), which was partially restored by pre-incubation of the hippocampal slices with IL-17 (Fig. 5B). These data demonstrate that IL-17 enhances synaptic plasticity during short-term learning. However, long-term memory trained IL-17-/- mice displayed similar LTP to WT controls (Fig. 5C), which is consistent with their normal performance in such paradigms (Fig. 4E and S9-10) and highlights additional/ compensatory mechanisms deployed in long-term cognition. This indicates a specific impact of IL-17 in these two dissociable forms of spatial information processing, both of which depend on the hippocampus (33).

The fact that animals deficient for GluR1 AMPA receptors display a very similar phenotype to that of IL-17-/- mice (30, 34), suggested a role of IL-17 (direct or indirect) in modulation of glutamatergic function. Consistently, we observed that IL-17-/- animals have a shifted input/output (I/O) curve post short-term Y-maze (but not at steady state) (Fig. 5D-E), associated with a reduction in the AMPAR/NMDAR ratio in CA1 glutamatergic neurons (Fig 5F), whereas their paired-pulse ratio remained unaffected (Fig 5G). Of note, the electrophysiological characterization obtained in IL-17-/- mice was phenocopied using TCRδ-/- mice (Fig. 6E, S13), further validating meningeal γδ T cells as the main source of IL-17 in the steady-state CNS.

IL-17 promotes glial BDNF production

Based on previous studies demonstrating that astrocytes and microglial cells constitutively express IL-17RA (35), we hypothesized that glial cells could be critical responders to IL-17 in our model, especially since astrocyte end-feet are in close contact with the meningeal areas, and have been suggested to act as sensors of the meningeal cytokine milieu (1). To address this hypothesis, we crossed IL-17RA$^{fl/fl}$ mice with specific Cre lines to generate mice where IL-17RA is conditionally deleted on astrocytes (using a constitutive GFAP-Cre model) or on the microglia (using an inducible CX3CR1-Cre model). However, none of the single conditional KO animals recapitulated the short-term cognitive deficits observed with mice deficient for IL-17 (Fig. S14), pointing to the potential existence of compensatory mechanisms. We then crossed the two lines to generate double conditional KO mice. While we observed a relative loss in the capacity to discriminate between the Novel and Other arms, this did not achieve the extent of IL-17-/- mice (Fig. S14), suggesting the involvement of additional cellular populations. In fact, neurons, pericytes, and endothelial cells are potential candidates to also respond to IL-17 (36–38).

To gain further molecular insight on the link between meningeal IL-17, glial cells and neuronal functions, we considered Brain Derived Neural Factor (BDNF) given that its expression is modulated by cytokines (20, 22); and it has been implicated in several learning and memory paradigms (39) especially through regulation of synaptic plasticity (40). Namely, mice deficient for BDNF display significant deficits in basal synaptic transmission characterized by an impaired LTP (41). We examined the effect of IL-17 on primary glial cultures and found increased BDNF production (Fig. 6A). Moreover, *ex vivo* analysis of the hippocampus showed significantly lower levels of BDNF in IL-17-/- animals compared to WT controls selectively after a short-term Y-maze (but not after a long-term MWM) paradigm (Fig. 6B). Furthermore, the incubation of hippocampal slices from IL-17-/- or TCRδ-/- mice with exogenous BDNF rescued their LTP and basal transmission deficits (Fig. 6C-E and Fig. S17); and, strikingly, an intracerebroventricular injection of BDNF restored short-term working memory in IL-17-/- mice (Fig. 6F). Collectively, these neurophysiology and behavioral data suggest a key role for glial BDNF as a molecular link between meningeal γδ17 T cells and hippocampal neuronal plasticity.

Discussion

The immune system has been traditionally regarded as a network of interacting cells and products critical for host defense against invading microbes and tumors. This notwithstanding, disease is a relatively rare manifestation and maintaining such a complex structure in homeostasis represents an important biological cost. In fact, the immune system is likely to have major physiological roles extending far beyond defending the host, as suggested by recent studies showing that immune cells can sense environmental signals and regulate physiological processes, such as nervous system function, metabolic homeostasis, thermogenesis, and tissue repair (15).

In this study we provide new clues on the evolutionary and functional link between the immune and nervous systems through three major advances: (i) we reveal a previously unknown meningeal-resident γδ T cell subset that accounts for essentially all the local IL-17

producing cells at steady state, (ii) we demonstrate that this subset regulates cognitive dissociation in the hippocampus in an IL-17-dependent manner, and (iii) we show evidence that IL-17 increases glial BDNF production and modulates neuronal synaptic plasticity in the hippocampus.

BDNF has been shown to be a key molecule in various learning and memory paradigms, such as the Y-maze and MWM (39, 42). Besides our *in vivo* data – restoring cognitive performance in the Y-Maze – we also show that BDNF rescues the LTP impairment observed in IL-17 -/- and TCRδ-/- mice. LTP is the main form of synaptic plasticity reflecting the activity of synaptic information storage processes, and has been often used as the gold standard cellular correlate of learning and memory in the hippocampus (43–47). Although these BDNF rescue experiments may not be physiologic, as often is the case with experimental manipulation/ perturbation of biological systems, we believe that they strongly supports, as a proof of concept, that BDNF can bypass the downstream mechanisms affected by the lack of IL-17 in the CNS. This notwithstanding, we do not rule out that other neurotransmitters may potentially contribute to the IL-17-mediated regulation of cognitive behavior.

Previous studies have demonstrated that astrocytes and microglial cells constitutively express IL-17RA and that this receptor is functional, as glial cell cultures produced chemokines in response to IL-17 treatment *in vitro* (35). Of note, astrocytes are in close contact with meningeal areas, and have been suggested to act as sensors of the meningeal cytokine milieu (22), integrating the signals from the meningeal immune system and transmitting these informations to the CNS. Our experiments based on the conditional deletion of IL-17RA on astrocytes and microglia revealed a complex system with various compensatory mechanisms still to be explored. For instance, pericytes and endothelial cells are potential candidates to also respond to IL-17 (36). A direct impact of IL-17 on neurons is also not excluded, as IL-17R expression has been observed under basal conditions in neural stem cells (48), neuronal progenitor cells (37) and dorsal root ganglion neurons (49, 50).

We show that most meningeal IL-17 producing T cells are Vγ6+ γδ T cells, which have been previously reported to infiltrate the lung, liver, tongue, dermis, fat and genital tract (27), from where they are unlikely to act on brain cognition. Instead, we propose a local effect from γδ17 T cells that likely colonize the meninges driven by CCR6, a chemokine receptor that they express at high levels and has been recently implicated in the migration of γδ17 T cells to the dermis (51). Importantly, we could abrogate short-term memory by neutralizing IL-17 *in situ* through intra-cerebro-ventricular injection of an anti-IL17 specific blocking antibody, a similar approach to the one previously used to demonstrate a role for meningeal IFN-γ on social behavior (18).

In this study, we used full IL-17 and γδ T cell knock-out mice, because the genetic ablation of γδ T cells or IL-17 does not allow tissue-specific targeting of the cells/ molecule. Moreover, there are currently no suitable tools to efficiently deplete IL-17 selectively in the γδ T cell lineage. To overcome these limitations, we took advantage of the embryonic origin of the Vγ6+ γδ17 T cell subset that resides in the meninges and generated bone marrow chimeras, i.e. injected adult bone marrow into irradiated adult hosts from the same genetic

wild-type background. As previously reported (26), this procedure allows to generate animals with a γδ T cell compartment mostly devoid of IL-17 producers. Importantly, these animals recapitulated the behavior of IL-17 or TCRδ full KO animals, showing a specific alteration of their short-term, but not long term memory. This dichotomy also rules out a general impact of irradiation on cognitive tasks when assessed more than 8 weeks post reconstitution. Of note, other publications in the field have employed this approach to dissect the impact of radioresistant versus radiosensitive immune cells on learning (22, 52).

Intriguingly, a deleterious effect of IL-17 on synaptic plasticity has been reported in the hippocampal dentate gyrus (DG), which exhibits pronounced differences in function and signal processing from our region of interest, CA1 (37). In particular, the I/O curves and the responses to paired pulse stimulation in DG are intrinsically distinct from CA1 (53, 54). Therefore, we believe that our report adds an unestablished role for IL-17 at steady-state in the CA1 region of the hippocampus which is distinct, but not contradictory to the current literature.

On the other hand, exacerbated levels of IL-17 have been associated to neuronal death and behavioral abnormalities. This was, for example, induced by intraperitoneal injections of LPS, as a non-physiological stimulus triggering systemic inflammation associated with cognitive impairements (55). Other recent work also reported a negative impact of maternal IL-17 on autism-like phenotype in offspring (56, 57). These studies concerned gut microbiota-dependent inflammatory IL-17 in pregnant mothers – likely mimicking viral infection – and its detrimental impact on neural developmental in the offspring. Furthermore, IL-17 produced by γδ T cells has also been shown to be deleterious in EAE (13) and stroke (12). We therefore propose a dual role for IL-17 in physiological *versus* pathological conditions. Whereas, as shown here, the steady-state (and microbiota-independent) production of IL-17 by meningeal γδ T cells promotes learning and memory, its exacerbated production (by γδ but also recruited CD4^{+} T cells) upon inflammation contributes to the pathogenesis of neuroinflammation and likely also to neurodegeneration, as recently suggested for Parkinson's disease (58, 59).

In sum, while the impact of the adaptive immune system on long-term memory has been under the spotlight (29), our work implicates innate-like γδ17 T cells, adding them to the portfolio of the immune populations infiltrating the central nervous system at steady state (60, 61). We thus propose a revised model that implicates resident meningeal innate-like γδ17 T cells in cognitive dissociation in the hippocampus (30, 34): they are selectively engaged in short-term memory, whereas adaptive αβ T cells seemingly control long-term memory upon recruitment to the meningeal spaces during the training period (20, 22). This provocative notion parallels the orchestration of an immune response to infection, where a rapid (within hours) engagement of innate-like (and often tissue-resident) T cells precedes the contribution of adaptive T cells, which take several days to clonally expand and migrate to the target tissues (2). Finally, as IL-17 was recently described as a neuromodulator of sensory response in *C. elegans* (62) and autism-like behavior in mice (56, 57), we expect this cytokine to impact other aspects of brain functions, thus defining new avenues to explore in neuroimmunology.

Material and methods

Study design

The goals of this study were to characterize meningeal resident γδ T cells and determine their impact on memory and learning under physiological conditions/steady state. Flow cytometry samples were pooled from 4 mice and a minimum of 4 independent experiments were performed. Behavioral testing was performed using TCRδ -/- and IL-17 -/-, with the respective wild-type littermate controls. A minimum of two independent experiments were performed for each behavior test, using a minimum of 8 mice per experimental group. Animals were randomized and the experimenter blinded to genotype for the duration of behavioral testing. The role of γδ17 T cells on glutamatergic synaptic plasticity was evaluated by performing field and patch-clamp electrophysiology recordings in hippocampal slices from IL-17 -/- and TCRδ -/- mice. A minimum of 3 mice were used per experimental group.

Animals

Animal research was conducted at the Instituto de Medicina Molecular. All experiments were approved by the animal ethics committee at the institute and performed according to national and European regulations. Rodents were purchased from Charles River (Spain).

All mice were from the C57BL/6 background, either bred in-house (WT, TCRδ-/-, IL- 17-/-, IL-1R-/-, IL-23R-/- and NOD1-/-), bred at IGC (Oeiras, Portugal) (TLR2-/- and TLR4-/-), bred at Mill Hills (London, UK) (IL-17aCreR26ReYFP), purchased from CharlesRiver (WT) or from the Jackson Laboratory (Caspase 1 -/-). When possible, mice used for experiments were littermates. Mice were bred in specific pathogen-free conditions and maintained in the SPF facility of IMM.WT Germ-Free (GF) mice were bred and maintained in the GF facility of IGC. When indicated, an antibiotic cocktail (streptomycin 5g/L, ampicillin 1g/L collistin 1g/L and vancomycin 0,5g/L; all from Sigma) was delivered in the drinking water supplemented with with 3% sucrose, (Sigma) *in utero* (by treating pregnant females) or after weaning. Control mice were given 3% sucrose in drinking water. Unless specified (uterus FACS characterization), all mice used were 10-24 week-old males.

Bone Marrow Chimeras

Bone marrow chimeras (WT→WT BMC) were generated as previously described (10). Briefly, C57BL/6J WT mice were lethelly irradiated (950 rad) and on the next day injected intravenously with a total of $5–10 \times 106$ whole bone marrow cells from C57BL/6J (Thy1.1+) donor mice. All BMCs were kept on antibiotics-containing water (2% Bactrim; Roche) for the first 4 weeks post-irradiation. The hematopoietic compartment was allowed to reconstitute for 8 weeks before the animals were used for experiments.

Flow cytometry

Mice were sacrificed with CO_2 and immediately transcardiacally perfused with ice- cold PBS. Meninges were collected and processed as previously described (7). Tongues, brains and uterus were cut into 2 mm^2 pieces and incubated for 30 minutes at 37°C with stirring in RPMI 5% fetal bovine serum (FBS) medium supplemented with collagenase D (1.5 mg/ml;

Roche) and and DNAse I (100 μg/mL, Roche). Supernatants were collected and live cells were isolated on a gradient of Percoll 70% - 30% (GE Healthcare). Spleens and cLNs were homogenized and washed in RPMI medium 10% FBS. Meninges, uterus and tongues were pooled from 3-5 mice, brains and spleens were analysed individually. FACS stainings were performed as previously described (32) using indicated monoclonal antibodies (mAbs) (Supplementary Table 2). Dead cells were excluded using LiveDead Fixable Viability Dye (Invitrogen). Samples were acquired using FACSFortessa (BD Biosciences). Data were analysed using FlowJo software (Tree Star).

Behavioral Tests

Mice were handled for 5 days before behavioral tests, which were performed in the following sequence: open-field (OF), elevated plus maze (EPM), Y-Maze and Morris water maze (MWM). Mazes were cleaned with a 30% ethanol solution between each trial. Animals were randomized and the experimenter blinded to genotype for the duration of behavioral testing. All behavioral tests were performed during the light phase between 8 a.m. and 6 p.m, under dim light, in a sound attenuated room. Mice movements were recorded and analyzed using the video-tracking software – SMART®.

Open Field. The OF was performed as previously described (63). *Elevated Plus Maze.* The EPM was performed as previously described (64). *Y-Maze.* The short-term Y-maze was performed as previously described (63). Briefly, this is in a two-trial recognition test in a Y-shaped maze with 3 arms (each with 35 cm length x 10 cm width x 20 cm height), angled at 120°; on the first trial (learning trial), the animal explored the maze for 10min with only two arms opened (start and other arm); after returning to his home cage for 1 h, the same animal was re-exposed to the maze for 5min (test trial) with the novel arm available. In the long-term Y-maze (adapted from (30)), mice were trained for a period of 5 days, 5 minutes per day. On day 6, animals were allowed to explore the 3 arms of the maze for 5 minutes for the test trial. The number of transitions was used to evaluate motor performances and the time spent exploring each arm was quantified. Discrimination ratio is calculated dividing time in the N or O arm, by the sum of the time in both arms (N+O). *Morris Water Maze.* The long-term MWM was performed as previously described (65) during five consecutive days and consisted of a four day acquisition phase and a one day probe test. During the acquisition phase each mouse was given four swimming trials per day (30-min intertrial interval). A trial consisted of allowing the mouse to explore and reach for the hidden platform. If the animal reached the platform before 60 sec, it was allowed to remain there for 10 sec; if the animal failed to find the target before 60 sec, it was manually guided to the platform, where it was allowed to remain for 20 sec. On the probe test, the platform was removed and animals were allowed to swim freely for 60 sec while recording the percentage of time spent on each quadrant. In the short-term MWM (adapted from (31) animals were trained on the same day, 7 trials per day ith and inter-trial interval of 30 s. One hour after the acquisition phase, animals were tested for 1 min.

Intracerebroventricular (i.c.v) injections

WT and IL17 -/- mice were administered BDNF (0.1 mg/mL, total volume of 3 μl), saline solution (PBS, total volume of 3 μl) or anti-mouse IL-17 (0.8 mg/mL, total volume of 5 μl)

(Clone 17F3, BioXCell) and IgG1 isotype control (0.8 mg/mL, total volume of 5 μl) (Clone MOPC-21) by i.c.v. injection as previously described (35). Briefly, mice were anesthetized under 1.5% isoflurane in 100% oxygen in a transparent acrylic chamber. After the induction, mice were moved out of the chamber to a stereotaxic frame, and isoflurane anesthesia was maintained. A single i.c.v was performed into the right ventricle of the brain, using the stereotaxic coordinates of 0.6 mm posterior, 1.2 mm lateral and 2.2 mm ventral to Bregma. A 10 μl hamilton syringe was used for i.c.v injection. Behavioral assessment was performed 24h after surgery in the Y-maze.

Proteomic analysis

Sample preparation. IL-17−/− and WT controls were sacrificed immediately after the Y-maze training by cervical dislocation followed by hippocampi isolation. The subproteome fractionation and protein precipitation of the hippocampi was performed as described in (66) and the protein pellets were resuspended in 2× Laemmli buffer (5% glycerol, 1.7% SDS, 100 mM DTT and bromophenol blue in 50 mM Tris Buffer at pH 6.8). Prior to ultracentrifugation a part of each homogenized sample (roughly 10%) was pooled per group. Total protein content was assessed with the commercial kit 2D Quant Kit (GE Healthcare) and 30 μg of the soluble fraction were used for SWATH-MS analysis. After denaturation at 95°C, samples were alkylated and subjected to in gel digestion using the short- GeLC approach (67). *IDA and SWATH acquisition and processing.* Samples were analyzed on a TripleTOF™ 5600 System (ABSciex®) in two phases: information-dependent acquisition (IDA) of the pooled samples for protein identification and SWATH acquisition of each individual sample fraction for quantification. A specific library of precursor masses and fragment ions was created by combining all files from the IDA experiments, and used for subsequent SWATH processing. Library was obtained using ProteinPilot™ software (v5.0, ABSciex®) searching against a *Mus musculus* database from SwissProt (download in July 2016). SWATH data processing was performed using SWATH™ processing plug-in for PeakView™ (v2.0.01, ABSciex®) as described in (67) adapted for the present samples. All the peptide that met the 1% FDR threshold in at least 3 replicates were retained and the levels of the proteins were estimated by summing the respective transitions and peptides that met the criteria established (an adaptation of (68)). For comparisons between experimental conditions, the protein levels were normalized to the total intensity of the sample.

The mass spectrometry proteomics data have been deposited to the ProteomeXchange Consortium via the PRIDE partner repository (69) with the dataset identifier PXD007574.

Bioinformatic analysis

The list of total identified entities from the proteomic analysis was uploaded into the DAVID 6.8 informatic tool, using the available Mus musculus database as background. Resulting clustered KEGG pathways with a enrichment score > 1.5 and p value and Benjamini score < 0.05 were selected.

Microbiome evaluation via 16S rRNA gene sequencing

Fecal samples were collected from animals and snap frozen and stored at −80°C as until microbial DNA extraction. Before extraction, samples were homogenized in 2 mL sterile

tubes containing 1mm of diameter autoclaved zirconia/silica beads (BioSpec Products), with the help of tissue homogenizer. Microbial genomic DNA was extracted using the QIAamp® Fast DNA Stool Mini kit (Qiagen). The 16S rRNA V4 amplicons and ITS1-spanning amplicons were both generated using the following Earth Microbiome Project benchmarked protocols. Amplicons were then sequenced using a 280-multiplex approach on a 2x250bp PE MiSeq run at Instituto Gulbenkian de Ciências (IGC) Genomics Unit (Oeiras, Portugal). Raw sequences were first loaded into the QIIME 1.9.1 pipeline using custom analysis scripts for analysis on the UBELIX Linux cluster of the University of Bern. Operational taxonomic units were picked using UCLUST with a 97% sequence identity threshold, using the default options as implemented in QIIME and followed by taxonomy assignment using the latest Greengenes database (greengenes.secondgenome.com). Calculation of the α- diversity (Observed OTUs, Simpson and Shannon indices), β-diversity (Bray–Curtis genus-level community dissimilarities, weighted and unweighted UniFrac-based PCoA), and statistical analysis of clustering using Mann–Whitney U-tests for alpha diversity and Adonis (PERMANOVA) for beta diversity to confirm that the strength and statistical significance of groups in the same distance metrics in the QIIME pipeline and phyloseq in R. The Q value package was implemented in MaAsLin to correct for multiple testing (BH-FDR correction, q value) of 0.05. After correction for a false discovery rate, $q < 0.05$ was considered significant.

Enzyme-linked immunosorbent assay (ELISA)

After the Y-maze or MWM, mice were sacrificed with CO2 and immediately transcardiacally perfused with ice-cold PBS. The meninges, hippocampi and prefrontal cortex were dissected and frozen in liquid nitrogen. Tissues samples were then homogenized by sonication in radioimmunoprecipitation assay (RIPA) buffer pH 8.0 (NaCl 150 mM, Tris-base 50 mM, EDTA 1 mM, Nonidet P40 1%, sodium dodecyl sulfate 0.1%, proteases inhibitors; Roche). Total protein content was quantified using the BioRad DC Protein Assay kit. Levels of BDNF were measured by ELISA, according to manufacturer's instructions (Promega).

Primary glial cultures

Astrocytes-enriched cultures were prepared from mice cerebral forebrain as previously reported (22). Briefly, newborn mice (0–3 days old) were sacrificed by decapitation and the brain was dissected in ice cold PBS inside a laminar flow chamber. Cells were dissociated in 4.5 g/L glucose Dulbecco's Modified Eagles Medium (DMEM) (Gibco), supplemented with 10% fetal bovine serum (FBS) (Gibco) and 1% antibiotic/antimycotic, and cultured in poly-D-lysine hydrobromide (10 μg/mL, Sigma). Cultures were maintained at 37°C in a humidified atmosphere (5% CO2) for 21 days and medium was replaced every 3–4 days. At 14 days *in vitro,* cultures were supplemented with IL-17 (10 ng/ml; Ebioscience). At the end of the culture, supernatants were collected for ELISA assays.

Electrophysiological fEPSPs recordings

IL17-/- mice and WT controls were sacrificed by cervical dislocation after Y-maze or MWM trainings. The brain was rapidly removed and the hippocampi were dissected free in ice-cold Krebs solution (124 mM NaCl; 3 mM KCl; 1.25mM NaH2PO4; 26 mM NaHCO3; 1 mM

MgSO4; 2 mM CaCl2 and 10 mM D-glucose), previously gassed with 95% O2 and 5% CO2, pH 7.4. 400 µM transverse hippocampal slices were obtained with a McIIwain tissue chopper and field excitatory postsynaptic potentials (fEPSPs) were recorded in stratum radiatum of the CA1 area as previously described (70). For recovery experiments, hippocampal slices were pre-incubated with IL17 (10ng/mL; Ebioscience) for 1 hour; or with BDNF (30 ng/mL; Amgen Inc) for 30min before LTP induction and remained in circulation up to the end of the experiment. After obtaining a stable 10 minutes baseline, Input/Output (I/O) curves, long term potentiation (LTP, 10c trains with 4 pulses at 100 Hz separated by 200 ms, induced at 0.5mV/ms) and paired-pulse facilitation (EPSC at 50 ms interpulse interval) were recorded. Recordings were performed at 32oC, 3 mL/min.

Patch-clamp experiments

Whole-cell patch-clamp experiments were performed in the voltage-clamp configuration (71), using a pipette solution containing (in mM): 117.5 cesium methanesulfonate, 15 CsCl, 10 tetraethylammonium chloride (TEACl), 8 NaCl, 10 HEPES, 0.25 EGTA, 4 MgATP, 0.3 NaGTP; the pH was adjusted to 7.3 with CsOH. For all experiments, slices were superfused with the oxygenated ACSF at 32 °C in the continuous presence of 50 µM picrotoxin (dissolved in Dimethylsulfoxide (DMSO), Sigma-Aldrich, France) to block GABAergic transmission. The Schaffer collateral pathway was stimulated at 0.10 Hz using electrodes (glass pipettes filled with ACSF) placed in the stratum radiatum. After a tight seal (> 1 GΩ) on the cell body of the selected neuron was obtained, whole-cell patch-clamp configuration was established, and cells were left to stabilize for approximately 2 min before recordings began. To calculate the AMPAR/NMDAR ratio, cells were held at −65 mV to record AMPAR EPSCs and at + 40 mV to record NMDAR EPSCs. AMPAR EPSCs amplitudes were calculated by averaging 30 consecutive EPSCs recorded at −65 mV and measuring the peak compared to the baseline. NMDAR EPSCs amplitudes were calculated by averaging 30 consecutive EPSCs recorded at + 40 mV and measuring the amplitude 60 ms after EPSC onset compared to the baseline.

Statistical analysis

The values presented are mean ± SEM of n independent experiments. To test the significance of the differences between 2 conditions, a Student's t test, Mann-whitney and F-Test were used. In statistical tests between 3 or more conditions, a one-way ANOVA or Kurskal-Wallis Test followed by a Bonferroni's or Dunnett's multiple comparison post hoc test as specified in the figure legends. P-values of < 0.05 were considered to be statistically significant.

Supplementary Material

Refer to Web version on PubMed Central for supplementary material.

Acknowledgements

References

1. Kipnis J, Gadani S, Derecki NC. Pro-cognitive properties of T cells. Nat Rev Immunol. 2012; 12:663–669. [PubMed: 22903149]

2. Weaver CT, Harrington LE, Mangan PR, Gavrieli M, Murphy KM. Th17: an effector CD4 T cell lineage with regulatory T cell ties. Immunity. 2006; 24:677–688. [PubMed: 16782025]

3. Ribot JC, deBarros A, Pang DJ, Neves JF, Peperzak V, Roberts SJ, Girardi M, Borst J, Hayday AC, Pennington DJ, Silva-Santos B. CD27 is a thymic determinant of the balance between interferon-gamma- and interleukin 17-producing gammadelta T cell subsets. Nat Immunol. 2009; 10:427–436. [PubMed: 19270712]

4. Jensen KD, Su X, Shin S, Li L, Youssef S, Yamasaki S, Steinman L, Saito T, Locksley RM, Davis MM, Baumgarth N, et al. Thymic selection determines gammadelta T cell effector fate: antigen-naive cells make interleukin-17 and antigen-experienced cells make interferon gamma. Immunity. 2008; 29:90–100. [PubMed: 18585064]

5. Munoz-Ruiz M, Ribot JC, Grosso AR, Goncalves-Sousa N, Pamplona A, Pennington DJ, Regueiro JR, Fernandez-Malave E, Silva-Santos B. TCR signal strength controls thymic differentiation of discrete proinflammatory gammadelta T cell subsets. Nat Immunol. 2016; 17:721–727. [PubMed: 27043412]

6. Ribot JC, Chaves-Ferreira M, d'Orey F, Wencker M, Goncalves-Sousa N, Decalf J, Simas JP, Hayday AC, Silva-Santos B. Cutting edge: adaptive versus innate receptor signals selectively control the pool sizes of murine IFN-gamma- or IL-17-producing gammadelta T cells upon infection. J Immunol. 2010; 185:6421–6425. [PubMed: 21037088]

7. Haas JD, Gonzalez FH, Schmitz S, Chennupati V, Fohse L, Kremmer E, Forster R, Prinz I. CCR6 and NK1.1 distinguish between IL-17A and IFN-gamma-producing gammadelta effector T cells. Eur J Immunol. 2009; 39:3488–3497. [PubMed: 19830744]

8. Munoz-Ruiz M, Sumaria N, Pennington DJ, Silva-Santos B. Thymic Determinants of gammadelta T Cell Differentiation. Trends Immunol. 2017; 38:336–344. [PubMed: 28285814]

9. Dandekar AA, O'Malley K, Perlman S. Important roles for gamma interferon and NKG2D in gammadelta T-cell-induced demyelination in T-cell receptor beta-deficient mice infected with a coronavirus. J Virol. 2005; 79:9388–9396. [PubMed: 16014902]

10. Sutton CE, Lalor SJ, Sweeney CM, Brereton CF, Lavelle EC, Mills KH. Interleukin-1 and IL-23 induce innate IL-17 production from gammadelta T cells, amplifying Th17 responses and autoimmunity. Immunity. 2009; 31:331–341. [PubMed: 19682929]

11. Shichita T, Sugiyama Y, Ooboshi H, Sugimori H, Nakagawa R, Takada I, Iwaki T, Okada Y, Iida M, Cua DJ, Iwakura Y, et al. Pivotal role of cerebral interleukin-17-producing gammadeltaT cells in the delayed phase of ischemic brain injury. Nat Med. 2009; 15:946–950. [PubMed: 19648929]

12. Benakis C, Brea D, Caballero S, Faraco G, Moore J, Murphy M, Sita G, Racchumi G, Ling L, Pamer EG, Iadecola C, et al. Commensal microbiota affects ischemic stroke outcome by regulating intestinal gammadelta T cells. Nat Med. 2016; 22:516–523. [PubMed: 27019327]

13. Pikor NB, Astarita JL, Summers-Deluca L, Galicia G, Qu J, Ward LA, Armstrong S, Dominguez CX, Malhotra D, Heiden B, Kay R, et al. Integration of Th17- and Lymphotoxin-Derived Signals Initiates Meningeal-Resident Stromal Cell Remodeling to Propagate Neuroinflammation. Immunity. 2015; 43:1160–1173. [PubMed: 26682987]

14. Ono T, Okamoto K, Nakashima T, Nitta T, Hori S, Iwakura Y, Takayanagi H. IL-17-producing gammadelta T cells enhance bone regeneration. Nat Commun. 2016; 7

15. Kohlgruber AC, Gal-Oz ST, LaMarche NM, Shimazaki M, Duquette D, Koay HF, Nguyen HN, Mina AI, Paras T, Tavakkoli A, von Andrian U, et al. gammadelta T cells producing interleukin-17A regulate adipose regulatory T cell homeostasis and thermogenesis. Nat Immunol. 2018; 19:464–474. [PubMed: 29670241]

16. Louveau A, Smirnov I, Keyes TJ, Eccles JD, Rouhani SJ, Peske JD, Derecki NC, Castle D, Mandell JW, Lee KS, Harris TH, et al. Structural and functional features of central nervous system lymphatic vessels. Nature. 2015; 523:337–341. [PubMed: 26030524]

17. Aspelund A, Antila S, Proulx ST, Karlsen TV, Karaman S, Detmar M, Wiig H, Alitalo K. A dural lymphatic vascular system that drains brain interstitial fluid and macromolecules. J Exp Med. 2015; 212:991–999. [PubMed: 26077718]

18. Filiano AJ, Xu Y, Tustison NJ, Marsh RL, Baker W, Smirnov I, Overall CC, Gadani SP, Turner SD, Weng Z, Peerzade SN, et al. Unexpected role of interferon-gamma in regulating neuronal connectivity and social behaviour. Nature. 2016; 535:425–429. [PubMed: 27409813]

19. Oetjen LK, Mack MR, Feng J, Whelan TM, Niu H, Guo CJ, Chen S, Trier AM, Xu AZ, Tripathi SV, Luo J, et al. Sensory Neurons Co-opt Classical Immune Signaling Pathways to Mediate Chronic Itch. Cell. 2017; 171:217–228 e213. [PubMed: 28890086]

20. Brombacher TM, Nono JK, De Gouveia KS, Makena N, Darby M, Womersley J, Tamgue O, Brombacher F. IL-13-Mediated Regulation of Learning and Memory. J Immunol. 2017; 198:2681–2688. [PubMed: 28202615]

21. Kipnis J, Cohen H, Cardon M, Ziv Y, Schwartz M. T cell deficiency leads to cognitive dysfunction: implications for therapeutic vaccination for schizophrenia and other psychiatric conditions. Proc Natl Acad Sci U S A. 2004; 101:8180–8185. [PubMed: 15141078]

22. Derecki NC, Cardani AN, Yang CH, Quinnies KM, Crihfield A, Lynch KR, Kipnis J. Regulation of learning and memory by meningeal immunity: a key role for IL-4. J Exp Med. 2010; 207:1067–1080. [PubMed: 20439540]

23. Hennessy E, Gormley S, Lopez-Rodriguez AB, Murray C, Cunningham C. Systemic TNF-alpha produces acute cognitive dysfunction and exaggerated sickness behavior when superimposed upon progressive neurodegeneration. Brain Behav Immun. 2017; 59:233–244. [PubMed: 27633985]

24. Monteiro S, Ferreira FM, Pinto V, Roque S, Morais M, de Sa-Calcada D, Mota C, Correia-Neves M, Cerqueira JJ. Absence of IFNgamma promotes hippocampal plasticity and enhances cognitive performance. Transl Psychiatry. 2016; 6:e707. [PubMed: 26731444]

25. Papotto PH, Ribot JC, Silva-Santos B. IL-17(+) gammadelta T cells as kick-starters of inflammation. Nat Immunol. 2017; 18:604–611. [PubMed: 28518154]

26. Haas JD, Ravens S, Duber S, Sandrock I, Oberdorfer L, Kashani E, Chennupati V, Fohse L, Naumann R, Weiss S, Krueger A, et al. Development of interleukin-17-producing gammadelta T cells is restricted to a functional embryonic wave. Immunity. 2012; 37:48–59. [PubMed: 22770884]

27. Carding SR, Egan PJ. Gammadelta T cells: functional plasticity and heterogeneity. Nat Rev Immunol. 2002; 2:336–345. [PubMed: 12033739]

28. Hirota K, Duarte JH, Veldhoen M, Hornsby E, Li Y, Cua DJ, Ahlfors H, Wilhelm C, Tolaini M, Menzel U, Garefalaki A, et al. Fate mapping of IL-17-producing T cells in inflammatory responses. Nat Immunol. 2011; 12:255–263. [PubMed: 21278737]

29. Kipnis J. Multifaceted interactions between adaptive immunity and the central nervous system. Science. 2016; 353:766–771. [PubMed: 27540163]

30. Sanderson DJ, Good MA, Skelton K, Sprengel R, Seeburg PH, Rawlins JN, Bannerman DM. Enhanced long-term and impaired short-term spatial memory in GluA1 AMPA receptor subunit knockout mice: evidence for a dual-process memory model. Learn Mem. 2009; 16:379–386. [PubMed: 19470654]

31. Bolding K, Rudy JW. Place learning in the Morris water task: making the memory stick. Learn Mem. 2006; 13:278–286. [PubMed: 16705134]

32. Kim SJ, Linden DJ. Ubiquitous plasticity and memory storage. Neuron. 2007; 56:582–592. [PubMed: 18031678]

33. Kitamura T, Ogawa SK, Roy DS, Okuyama T, Morrissey MD, Smith LM, Redondo RL, Tonegawa S. Engrams and circuits crucial for systems consolidation of a memory. Science. 2017; 356:73–78. [PubMed: 28386011]

34. Reisel D, Bannerman DM, Schmitt WB, Deacon RM, Flint J, Borchardt T, Seeburg PH, Rawlins JN. Spatial memory dissociations in mice lacking GluR1. Nat Neurosci. 2002; 5:868–873. [PubMed: 12195431]

35. Das Sarma J, Ciric B, Marek R, Sadhukhan S, Caruso ML, Shafagh J, Fitzgerald DC, Shindler KS, Rostami A. Functional interleukin-17 receptor A is expressed in central nervous system glia and upregulated in experimental autoimmune encephalomyelitis. J Neuroinflammation. 2009; 6:14. [PubMed: 19400960]

36. Kang Z, Altuntas CZ, Gulen MF, Liu C, Giltiay N, Qin H, Liu L, Qian W, Ransohoff RM, Bergmann C, Stohlman S, et al. Astrocyte-restricted ablation of interleukin-17-induced Act1-mediated signaling ameliorates autoimmune encephalomyelitis. Immunity. 2010; 32:414–425. [PubMed: 20303295]

37. Liu Q, Xin W, He P, Turner D, Yin J, Gan Y, Shi FD, Wu J. Interleukin-17 inhibits adult hippocampal neurogenesis. Sci Rep. 2014; 4

38. Liu R, Lauridsen HM, Amezquita RA, Pierce RW, Jane-Wit D, Fang C, Pellowe AS, Kirkiles-Smith NC, Gonzalez AL, Pober JS. IL-17 Promotes Neutrophil-Mediated Immunity by Activating Microvascular Pericytes and Not Endothelium. J Immunol. 2016; 197:2400–2408. [PubMed: 27534549]

39. Hall J, Thomas KL, Everitt BJ. Rapid and selective induction of BDNF expression in the hippocampus during contextual learning. Nat Neurosci. 2000; 3:533–535. [PubMed: 10816306]

40. Lu B, Nagappan G, Guan X, Nathan PJ, Wren P. BDNF-based synaptic repair as a disease-modifying strategy for neurodegenerative diseases. Nat Rev Neurosci. 2013; 14:401–416. [PubMed: 23674053]

41. Patterson SL, Abel T, Deuel TA, Martin KC, Rose JC, Kandel ER. Recombinant BDNF rescues deficits in basal synaptic transmission and hippocampal LTP in BDNF knockout mice. Neuron. 1996; 16:1137–1145. [PubMed: 8663990]

42. Choy KH, de Visser Y, Nichols NR, van den Buuse M. Combined neonatal stress and young-adult glucocorticoid stimulation in rats reduce BDNF expression in hippocampus: effects on learning and memory. Hippocampus. 2008; 18:655–667. [PubMed: 18398848]

43. Morris RG, Anderson E, Lynch GS, Baudry M. Selective impairment of learning and blockade of long-term potentiation by an N-methyl-D-aspartate receptor antagonist, AP5. Nature. 1986; 319:774–776. [PubMed: 2869411]

44. Bliss TV, Collingridge GL. A synaptic model of memory: long-term potentiation in the hippocampus. Nature. 1993; 361:31–39. [PubMed: 8421494]

45. Lisman J, Cooper K, Sehgal M, Silva AJ. Memory formation depends on both synapse-specific modifications of synaptic strength and cell-specific increases in excitability. Nat Neurosci. 2018; 21:309–314. [PubMed: 29434376]

46. Lynch MA. Long-term potentiation and memory. Physiol Rev. 2004; 84:87–136. [PubMed: 14715912]

47. Malenka RC. The long-term potential of LTP. Nat Rev Neurosci. 2003; 4:923–926. [PubMed: 14595403]

48. Li Z, Li K, Zhu L, Kan Q, Yan Y, Kumar P, Xu H, Rostami A, Zhang GX. Inhibitory effect of IL-17 on neural stem cell proliferation and neural cell differentiation. BMC Immunol. 2013; 14

49. Segond von Banchet G, Boettger MK, Konig C, Iwakura Y, Brauer R, Schaible HG. Neuronal IL-17 receptor upregulates TRPV4 but not TRPV1 receptors in DRG neurons and mediates mechanical but not thermal hyperalgesia. Mol Cell Neurosci. 2013; 52:152–160. [PubMed: 23147107]

50. Richter F, Natura G, Ebbinghaus M, von Banchet GS, Hensellek S, Konig C, Brauer R, Schaible HG. Interleukin-17 sensitizes joint nociceptors to mechanical stimuli and contributes to arthritic pain through neuronal interleukin-17 receptors in rodents. Arthritis Rheum. 2012; 64:4125–4134. [PubMed: 23192794]

51. McKenzie DR, Kara EE, Bastow CR, Tyllis TS, Fenix KA, Gregor CE, Wilson JJ, Babb R, Paton JC, Kallies A, Nutt SL, et al. IL-17-producing gammadelta T cells switch migratory patterns between resting and activated states. Nat Commun. 2017; 8

52. Garre JM, Silva HM, Lafaille JJ, Yang G. CX3CR1(+) monocytes modulate learning and learning-dependent dendritic spine remodeling via TNF-alpha. Nat Med. 2017; 23:714–722. [PubMed: 28504723]

53. Trieu BH, Kramar EA, Cox CD, Jia Y, Wang W, Gall CM, Lynch G. Pronounced differences in signal processing and synaptic plasticity between piriform-hippocampal network stages: a prominent role for adenosine. J Physiol. 2015; 593:2889–2907. [PubMed: 25902928]

54. Sharvit A, Segal M, Kehat O, Stork O, Richter-Levin G. Differential modulation of synaptic plasticity and local circuit activity in the dentate gyrus and CA1 regions of the rat hippocampus by corticosterone. Stress. 2015; 18:319–327. [PubMed: 25815975]

55. Sun J, Zhang S, Zhang X, Dong H, Qian Y. IL-17A is implicated in lipopolysaccharide-induced neuroinflammation and cognitive impairment in aged rats via microglial activation. J Neuroinflammation. 2015; 12

56. Kim S, Kim H, Yim YS, Ha S, Atarashi K, Tan TG, Longman RS, Honda K, Littman DR, Choi GB, Huh JR. Maternal gut bacteria promote neurodevelopmental abnormalities in mouse offspring. Nature. 2017; 549:528–532. [PubMed: 28902840]

57. Choi GB, Yim YS, Wong H, Kim S, Kim H, Kim SV, Hoeffer CA, Littman DR, Huh JR. The maternal interleukin-17a pathway in mice promotes autism-like phenotypes in offspring. Science. 2016; 351:933–939. [PubMed: 26822608]

58. Storelli E, Cassina N, Rasini E, Marino F, Cosentino M. Do Th17 Lymphocytes and IL-17 Contribute to Parkinson's Disease? A Systematic Review of Available Evidence. Front Neurol. 2019; 10:13. [PubMed: 30733703]

59. Liu Z, Qiu AW, Huang Y, Yang Y, Chen JN, Gu TT, Cao BB, Qiu YH, Peng YP. IL-17A exacerbates neuroinflammation and neurodegeneration by activating microglia in rodent models of Parkinson's disease. Brain Behav Immun. 2019

60. Korin B, Ben-Shaanan TL, Schiller M, Dubovik T, Azulay-Debby H, Boshnak NT, Koren T, Rolls A. High-dimensional, single-cell characterization of the brain's immune compartment. Nat Neurosci. 2017; 20:1300–1309. [PubMed: 28758994]

61. Kwong B, Rua R, Gao Y, Flickinger J Jr, Wang Y, Kruhlak MJ, Zhu J, Vivier E, McGavern DB, Lazarevic V. T-bet-dependent NKp46(+) innate lymphoid cells regulate the onset of TH17-induced neuroinflammation. Nat Immunol. 2017; 18:1117–1127. [PubMed: 28805812]

62. Chen C, Itakura E, Nelson GM, Sheng M, Laurent P, Fenk LA, Butcher RA, Hegde RS, de Bono M. IL-17 is a neuromodulator of Caenorhabditis elegans sensory responses. Nature. 2017; 542:43–48. [PubMed: 28099418]

63. Coelho JE, Alves P, Canas PM, Valadas JS, Shmidt T, Batalha VL, Ferreira DG, Ribeiro JA, Bader M, Cunha RA, do Couto FS, Lopes LV. Overexpression of Adenosine A2A Receptors in Rats: Effects on Depression, Locomotion, and Anxiety. Front Psychiatry. 2014; 5:67. [PubMed: 24982640]

64. Kulikov AV, Fursenko DV, Khotskin NV, Bazovkina DV, Kulikov VA, Naumenko VS, Bazhenova EY, Popova NK. Spatial learning in the Morris water maze in mice genetically different in the predisposition to catalepsy: the effect of intraventricular treatment with brain-derived neurotrophic factor. Pharmacol Biochem Behav. 2014; 122:266–272. [PubMed: 24780503]

65. Batalha VL, Pego JM, Fontinha BM, Costenla AR, Valadas JS, Baqi Y, Radjainia H, Muller CE, Sebastiao AM, Lopes LV. Adenosine A(2A) receptor blockade reverts hippocampal stress-induced deficits and restores corticosterone circadian oscillation. Mol Psychiatry. 2013; 18:320–331. [PubMed: 22371048]

66. Anjo. Neuromethods. Current Proteomic Approaches Applied to Brain FunctionHumana Press; New York, NY: 2017.

67. Anjo CS, Manadas B. Short GeLC-SWATH: a fast and reliable quantitative approach for proteomic screenings. Proteomics. 2015; 15:757–762. [PubMed: 25418953]

68. Collins BC, Gillet LC, Rosenberger G, Rost HL, Vichalkovski A, Gstaiger M, Aebersold R. Quantifying protein interaction dynamics by SWATH mass spectrometry: application to the 14-3-3 system. Nat Methods. 2013; 10:1246–1253. [PubMed: 24162925]

69. Vizcaino JA, Csordas A, del-Toro N, Dianes JA, Griss J, Lavidas I, Mayer G, Perez-Riverol Y, Reisinger F, Ternent T, Xu QW, et al. 2016 update of the PRIDE database and its related tools. Nucleic Acids Res. 2016; 44:D447–456. [PubMed: 26527722]

70. Ferreira DG, Temido-Ferreira M, Vicente Miranda H, Batalha VL, Coelho JE, Szego EM, Marques-Morgado I, Vaz SH, Rhee JS, Schmitz M, Zerr I, et al. alpha-synuclein interacts with PrP(C) to induce cognitive impairment through mGluR5 and NMDAR2B. Nat Neurosci. 2017; 20:1569–1579. [PubMed: 28945221]

71. Temido-Ferreira M, Ferreira DG, Batalha VL, Marques-Morgado I, Coelho JE, Pereira P, Gomes R, Pinto A, Carvalho S, Canas PM, Cuvelier L, et al. Age-related shift in LTD is dependent on neuronal adenosine A2A receptors interplay with mGluR5 and NMDA receptors. Mol Psychiatry. 2018
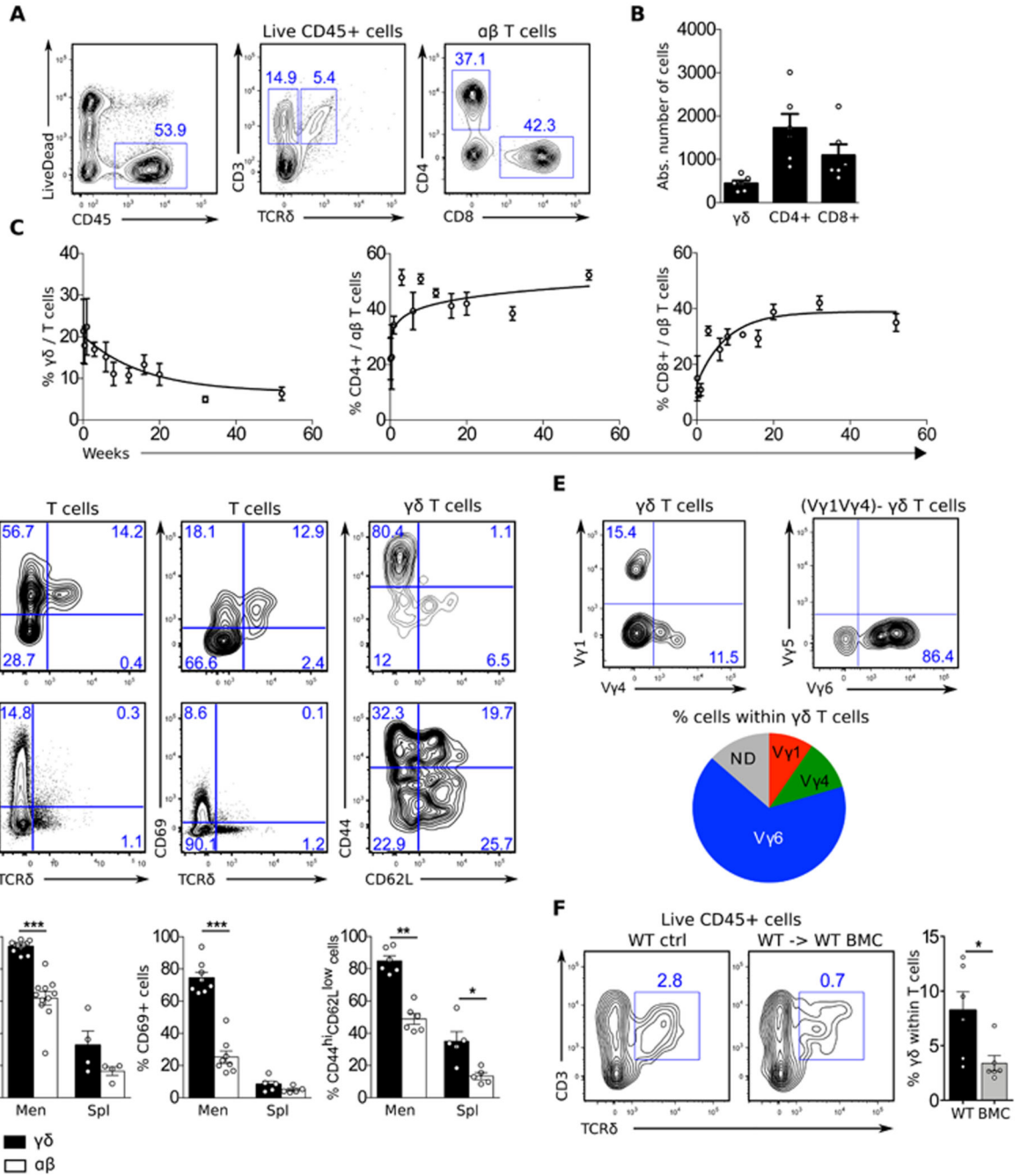
Figure 1. Foetal derived γδ T cells infiltrate the meninges from birth.
Meningeal cell suspensions were prepared from 8-20 weeks-old C57BL/6J WT and *Il17a*[Cre]
R26R[eYFP] mice (**A-B; D-E**), 0-52 weeks-old C57BL/6J WT mice (**C**), and 20 weeks-old
WT and WT → WT bone marrow chimeras (BMC) mice (**G**). Samples were analysed for
the expression of indicated surface (CD45, CD3, TCRδ, CD4, CD8, Vγ1, Vγ4, Vγ5, Vγ6,
CD27 and CCR6) and intracellular (RORgt, Tbet, IL-17 and IFN-γ) markers. Live cells
were gated using LiveDead Fixable Viability Dye as shown in **A**. Dot plots represents cell
populations from indicated gates. Histograms depicts percentages or absolute numbers from

indicated populations. Meningeal spaces were pooled from 4 mice. Spleens were analysed from individual mice. Results are representative of 4-7 independent experiments. Error bars, mean + s.e.m. * P<0.05, **P<0.01, ***P<0.001 as calculated by student T-test (parametric) or Mann-Whitney test (non parametric).
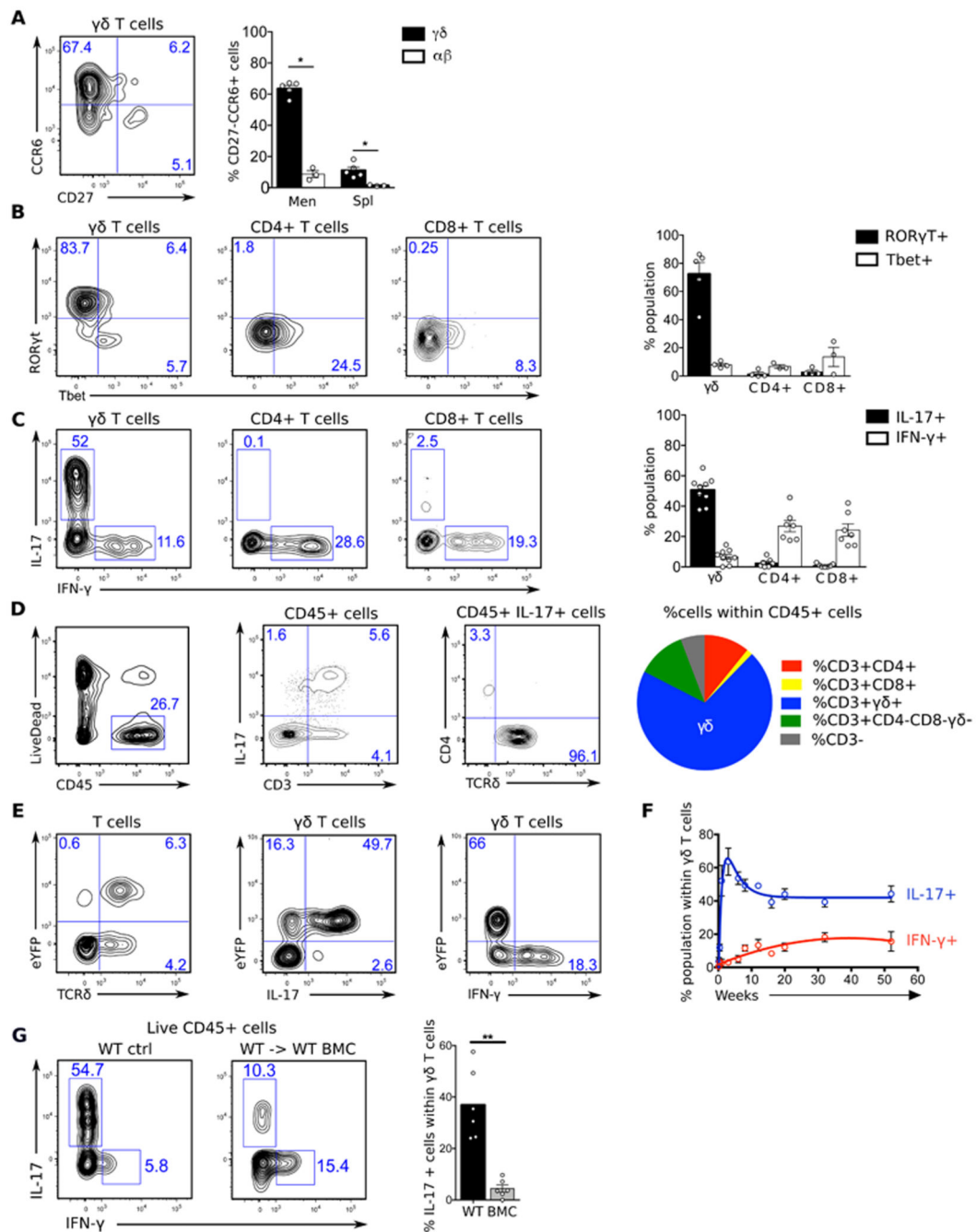
Figure 2. Meningeal γδ T cells are biased towards IL-17 production.

Meningeal cell suspensions were prepared from 8-20 weeks-old C57BL/6J WT and *Il17a*^Cre R26R^eYFP mice (**A-E**), 0-52 weeks-old C57BL/6J WT mice (**G**), and 20 weeks-old WT and WT → WT bone marrow chimeras (BMC) mice (**F**). Samples were analysed for the expression of indicated surface (CD45, CD3, TCRδ, CD4, CD8, Vγ1, Vγ4, Vγ5, Vγ6, CD27 and CCR6) and intracellular (RORgt, Tbet, IL-17 and IFN-γ) markers. Live cells were gated using LiveDead Fixable Viability Dye as shown in **A**. Dot plots represents cell populations from indicated gates. Histograms depicts percentages or absolute numbers from

indicated populations. Meningeal spaces were pooled from 4 mice. Spleens were analysed from individual mice. Results are representative of 4-7 independent experiments. Error bars, mean + s.e.m. * P<0.05, **P<0.01, as calculated by Mann-Whitney test.
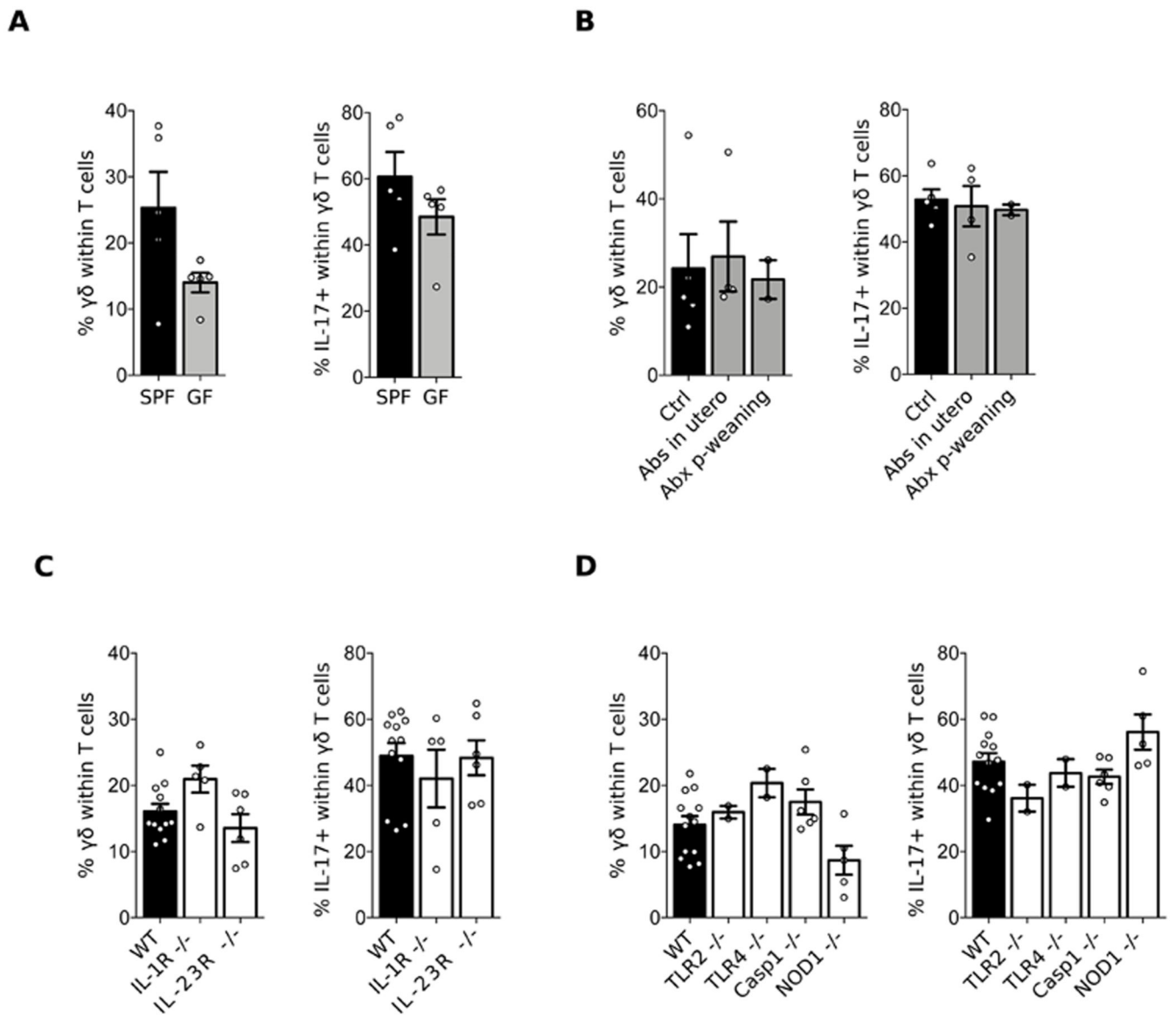
A

B

C

D

Figure 3. Meningeal γδ T cell homeostasis is independent of inflammatory signals
Cell suspensions were prepared from the meninges of 8-12 weeks-old C57BL/6J WT mice,
bred in a Specific Pathogen Free (SPF) **(A-D)** versus Germ Free (GF) **(A)** environment,
treated or not with an antibiotic cocktail **(B)**, and compared to IL-1R-/-, IL-23R-/- **(C)**,
TLR2-/-, TLR4-/-, Caspase 1-/- and NOD1-/- mice **(D)**. Percentages of γδ T cells and IL-17
producers were analysed by FACS as illustrated in Fig. 1. Results are representative of 2-4
independent experiments.

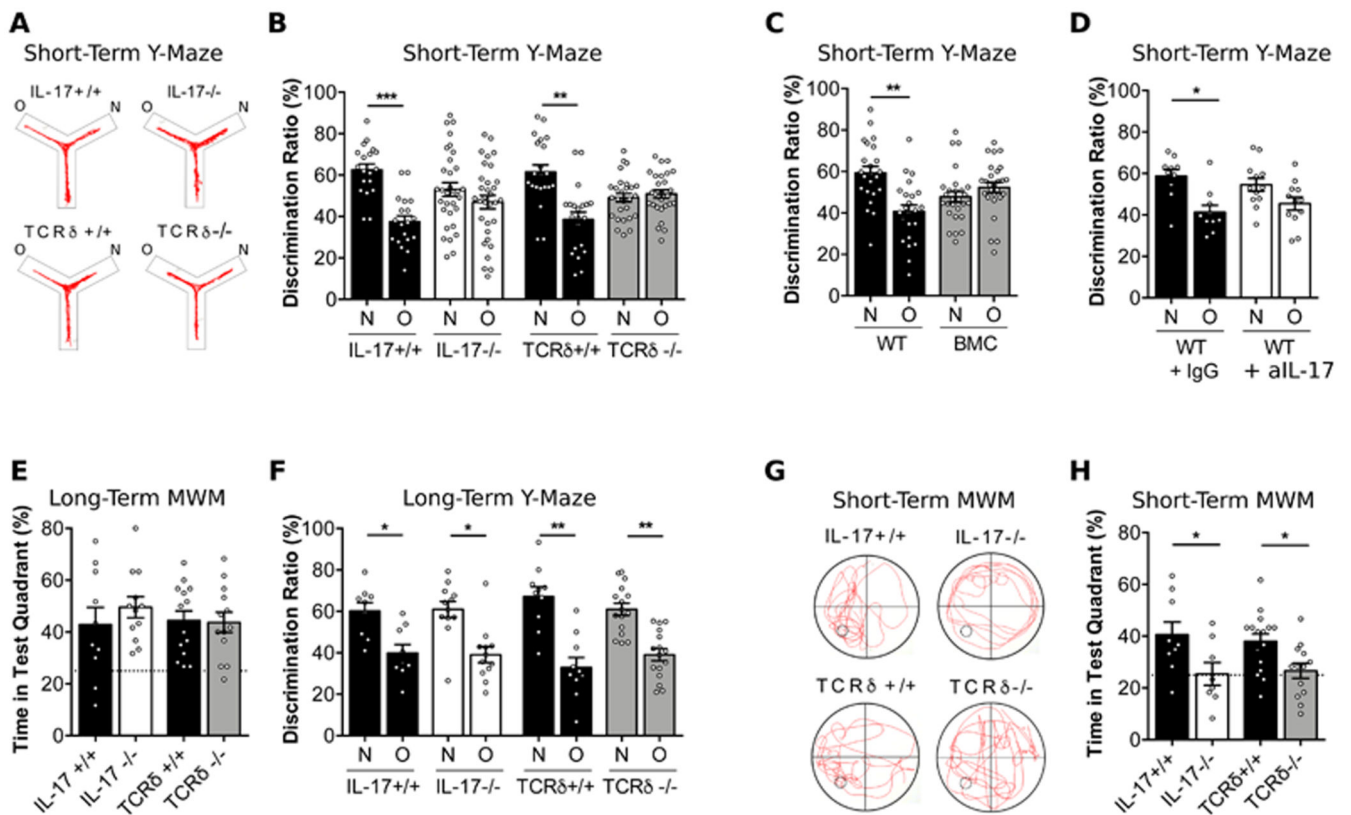**Figure 4. γδ T cells producing IL-17 are required for short-term memory.**
(A) Representative track line from indicated animals exploring the short-term Y-maze. **(B-D)** Cognitive performance in the short-term Y-maze evaluated by discrimination ratio between the novel arm (N) *versus* the other arm (O) of IL-17-/-, TCRδ-/- compared to respective littermate controls (n=21-32) **(B)**, WT → WT bone marrow chimeras (BMC) mice (n=23-27) **(C)** and WT after intra-cerebro-ventricular injection of isotype control (IgG) or anti-IL-17 (aIL-17) (n=10-12) **(D)**. **(E)** Percentages of swimming time in the test quadrant of IL-17-/- and TCRδ-/- and respective littermate controls during the probe test of the long-term Morris Water Maze (MWM) (n=10-14). **(F)** Cognitive performance in the long-term Y-maze evaluated by discrimination ratio between the novel arm (N) *versus* the other arm (O) of IL-17-/-, TCRδ-/- compared to respective littermate controls (n=10-16). **(G)** Representative track line from indicated animals exploring the short-term Morris Water Maze (MWM) during the probe test, after a training phase with a platform in the lower left quadrant of the pool. **(H)** Corresponding percentages of time spent in the test quadrant of IL-17-/- and TCRδ-/- and respective littermate controls (n=8-16). Results are representative of 2-3 independent experiments in male mice. Error bars, mean + s.e.m. **P<0.05; **P<0.0; ***P<0.001. Paired Student's t-test and One-way ANOVA followed by Bonferroni's multiple comparison test were used to analyse discrimination ratio (%) and Time in quadrant (%) respectively.
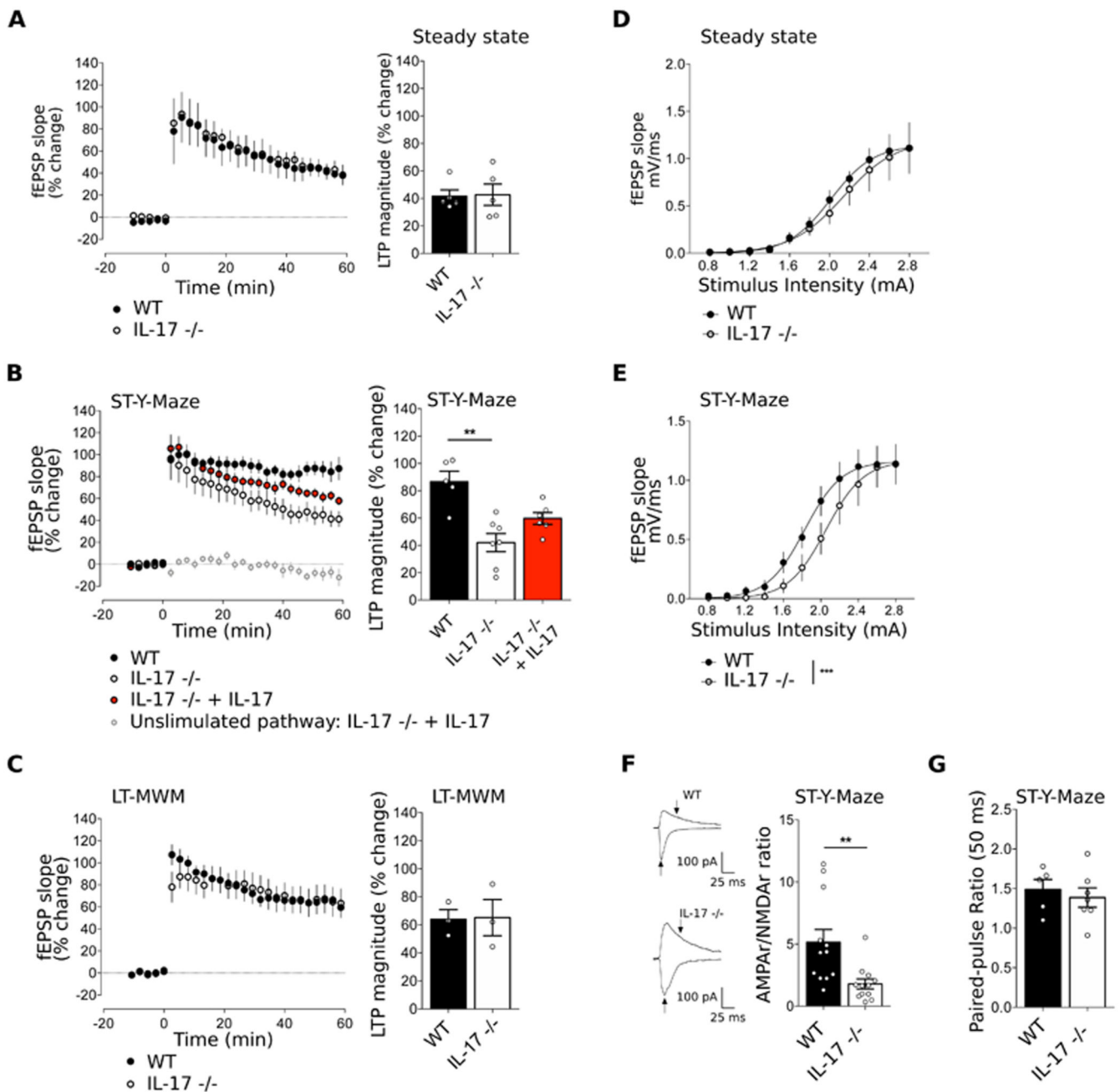
Figure 5. IL-17 modulates synaptic plasticity and AMPA/NMDA ratio upon a short-term memory task.
(A-C) Time course (left panels) and magnitude (right panels) of LTP induced by theta-burst stimulation (TBS) in hippocampal slices from WT and IL-17-/- mice at steady state **(A)**, after training in the short-term Y-Maze **(B)** and after training in the long-term MWM **(C)**. When indicated, hippocampal slices from IL-17-/- mice were supplemented with IL-17 (10ng/mL) (n=3-7, Kruskal-Wallis test followed by Dunn's multiple comparisons test). **(D-E)** Input/Output (I/O) curves corresponding to the fEPSP slope evoked by different stimulation intensities (0.8-2.8 mA) of IL-17-/- compared to WT mice at steady state **(D)**

and after training in the short-term Y-maze test **(E)** n=5-7, F-test. **(F)** Representative traces of EPSCs recorded at −70 mV and + 40 mV in neurons from WT and IL-17 -/- mice after training in the short-term Y-maze (left panels). Arrows indicate the amplitudes considered to calculate AMPAR/NMDAR ratio, depicted in the right panel. n=11-12, unpaired T-test. **(G)** Paired Pulse Facilitation, EPSCs at 50 ms interpulse intervals in WT and IL-17-/- after Y-maze (n=5-7, Mann-Whitney test). Data are mean ± s.e.m. **P<0.01, ***P<0.001.
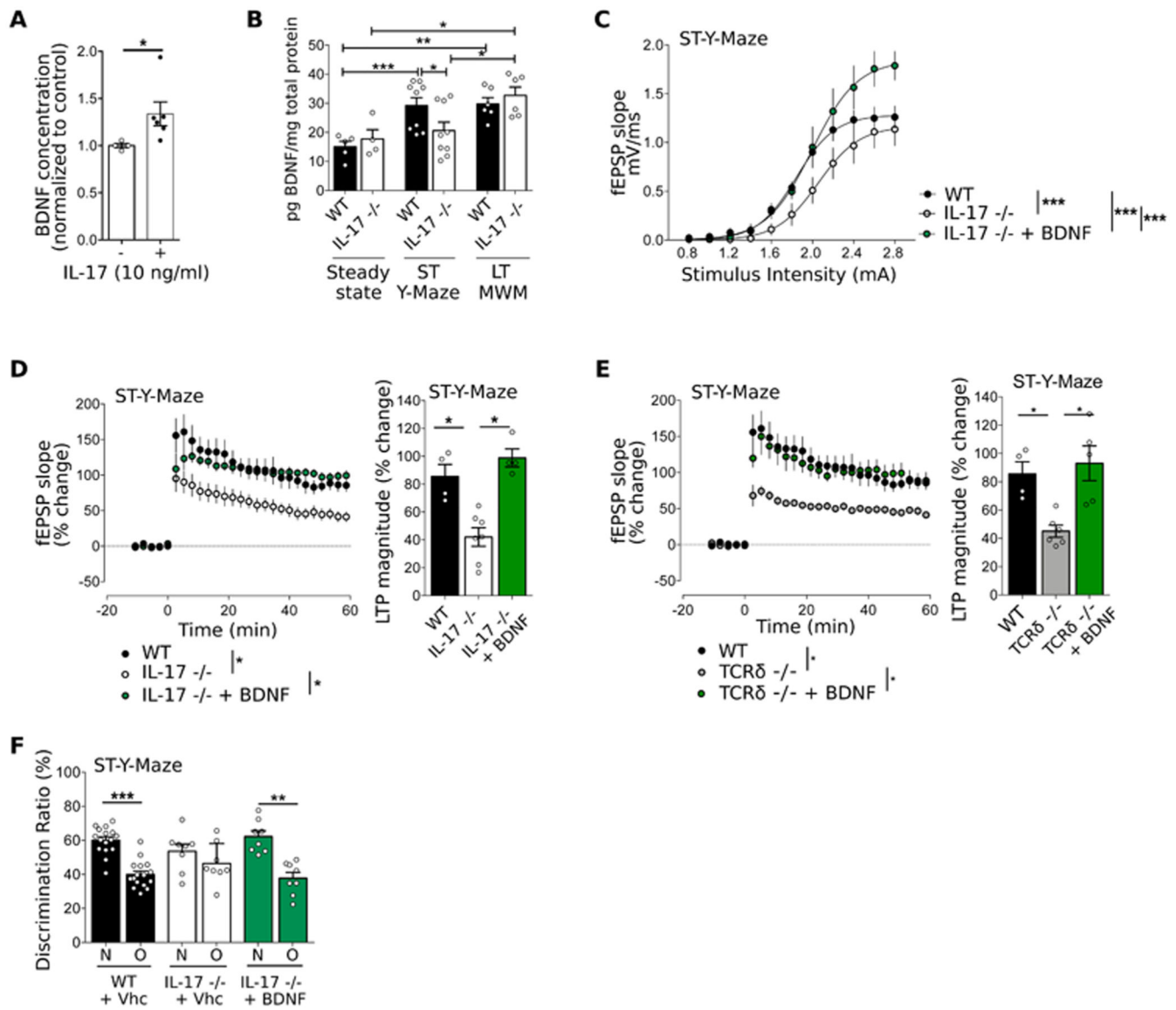
Figure 6. IL-17 promotes glial Brain-Derived Neurotrophic Factor (BDNF) production.
(A) BDNF concentration in mixed glial cultures supplemented with IL-17 normalized to the control condition (n=4-6, Mann-Whitney test). **(B)** BDNF concentration in the hippocampus at steady state, after short-term Y-Maze test and after long-term MWM test (n=4-9, Mann-Whitney test). **(C)** I/O curves corresponding to the fEPSP slope evoked by different stimulation intensities (0.8-3.0 mA) of WT, IL-17-/- IL-17-/- supplemented with BDNF (30 ng/mL) after short-term Y-maze test (n=5-6, F-test). **(D-E)** Time course (left panel) and magnitude (right panel) of LTP induced by TBS in CA1 region of hippocampal slices of **(D)** WT, IL-17 -/- and IL-17-/- supplemented with BDNF (30 ng/mL) and **(E)** WT, TCRδ-/- and TCRδ-/- supplemented with BDNF (30 ng/mL) after short-term Y-Maze test (n=4-7, Kruskal-Wallis test followed by Dunn's multiple comparisons test.). Raw data from IL-17 -/- in panel C and D are adapted from Fig 3B and E. Data from WT is the same in panels D and E. **(E)** Cognitive performance in Y-Maze evaluated by discrimination ratio between N *versus*

O of WT and IL-17-/- mice tested after ICV injection of PBS (vehicle, vhc) or BDNF (n=8-16, Paired Student's t-test). Results are representative of 2-5 independent experiments. Data are mean ± s.e.m, *P<0.05; **P<0.01; ***P<0.001.